Status of the Mu2e experiment

S. Giovannella[1,a] on behalf of the Mu2e Collaboration

[1] *Laboratori Nazionali di Frascati dell'INFN, via Enrico Fermi 40, 00044 Frascati, Italy*

Abstract. The Mu2e experiment at Fermilab searches for the charged-lepton flavor violating neutrino-less conversion of a negative muon into an electron in the field of an aluminum nucleus. The dynamics of such a process is well modelled by a two-body decay, resulting in a mono-energetic electron with an energy slightly below the muon rest mass. If no events are observed, in three years of running Mu2e will improve the current limit by four orders of magnitude. Such a charged lepton flavor-violating reaction probes new physics at a scale inaccessible with direct searches at either present or planned high energy colliders. The experiment both complements and extends the current search for muon decay to electron-photon at MEG and searches for new physics at the LHC. This paper focuses on the physics motivation, the design and the status of the experiment.

1 Introduction

Differently from their hadronic counterpart, charged lepton flavor transitions are not allowed in the Standard Model (SM) with massless neutrinos. Even including neutrino mass, charged lepton flavor violation (CLFV) processes are extremely suppressed in the SM, with rates smaller than 10^{-50} [1]. On the other hand, a broad variety of new physics Beyond the Standard Model (SUSY, Leptoquarks, GUT, ...), predicts significantly larger rates, within the reach of next generation of CLFV experiments [2]. Because of the negligible background, any CLFV experimental detection would be a clear indication of new physics.

Searches in muon channels are of particular interest because of their high rates and the possibility of carrying out clean measurements free of hadronic corrections in the calculation. Comparison of current limit and expectations from next generation experiment with other channels are reported in Fig. 1. The experimental search for CLFV with muons ($\mu \to e\gamma$, $\mu \to 3e$, and $\mu N \to eN$, *i.e.* the muon to electron conversion in the field of a nucleus) is progressing extremely fast in the last decades. Current best limits are BR($\mu \to e\gamma$) $< 4.2 \times 10^{-13}$ at 90 % C.L. (MEG [3]) and $R_{\mu e} < 7 \times 10^{-13}$ (SINDRUM-II [4]). A solid international program exists with the MEG upgrade [5] underway, a proposed $\mu \to 3e$ experiment at PSI (Mu3e [6]) and with the approved programs on the muon to electron conversion at FNAL (Mu2e) [7] and J-PARC (COMET/DeeMe) [8, 9].

Process	Current Limit	Next Generation exp
$\tau \to \mu\eta$	BR < 6.5 E-8	10^{-9} - 10^{-10} (Belle II)
$\tau \to \mu\gamma$	BR < 6.8 E-8	
$\tau \to \mu\mu\mu$	BR < 3.2 E-8	
$\tau \to eee$	BR < 3.6 E-8	
$K_L \to e\mu$	BR < 4.7 E-12	
$K^+ \to \pi^+ e^- \mu^+$	BR < 1.3 E-11	
$B^0 \to e\mu$	BR < 7.8 E-8	
$B^+ \to K^+ e\mu$	BR < 9.1 E-8	
$\mu^+ \to e^+\gamma$	BR < 4.2 E-13	10^{-14} (MEG)
$\mu^+ \to e^+e^+e^-$	BR < 1.0 E-12	10^{-16} (PSI)
$\mu N \to eN$	$R_{\mu e}$ < 7.0 E-13	10^{-17} (Mu2e, COMET)

Figure 1. Current best limits on CLFV searches and expectations from next generation experiments.

2 The Mu2e Experiment

The goal of the Mu2e experiment is to improve by four orders of magnitude the best previous measurement and reach a single event sensitivity of 3×10^{-17} on $R_{\mu e}$, the rate of neutrino-less conversion of a muon into an electron in the field of a nucleus with respect to the dominant muon capture process. The experimental technique consists of a high intensity beam of low momentum muons stopped in an aluminum target and trapped in orbit around the nucleus, with a lifetime in the bound state of $\tau_\mu = 864$ ns. The distinctive signature of the conversion electron (CE) is a mono-energetic electron with momentum very close to the muon rest mass, $E_{CE} = 104.96$ MeV (Fig. 2). Muons stopped on aluminium have a 39% probability of undergoing a three-body decay when orbiting around the nucleus. The electron spectrum of this Decay-In-Orbit (DIO) process substantially differs from that of free decay, due to the presence of a large recoil tail that falls rapidly as the electron energy approaches the kinematical endpoint. The CE line has to be distinguished, with a high momentum res-

[a] e-mail: simona.giovannella@lnf.infn.it

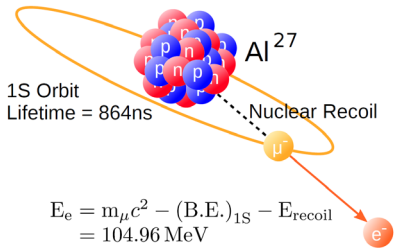

Figure 2. Drawing of the muon to electron conversion process.

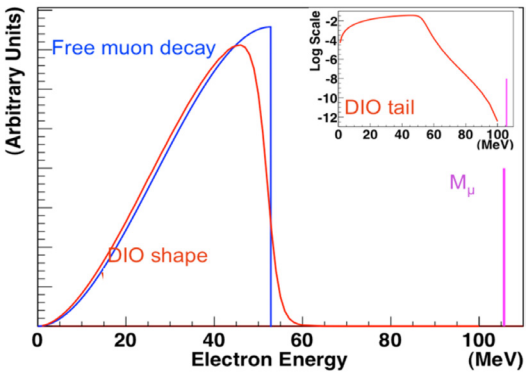

Figure 3. Energy spectrum for electrons produced from muon decays in orbit. An ideal resolution is assumed.

olution detector, from the DIO electron spectrum, Fig. 3.

Apart from the DIO contribution, an additional background source comes from the radiative pion capture (RPC), $\pi + N \rightarrow \gamma + N'$. Here, the electron positron pair, produced either by internal or external conversion, becomes a source of fake CE candidates when the e^- momentum is in the selection window.

In order to reach the required sensitivity, the experiment has to collect 10^{18} stopped muons with a number of background events less than 0.5. These considerations have driven the design strategy of Mu2e, based on four key elements:

1. A high intensity muon beam
   The goal is to increase the muon intensity by 10^4 w.r.t. previous experiments to reach 10^{11} muons/s on target. This is obtained combining a high rate particle production and a curved solenoidal system to create a transport channel that selects both charge and momentum.

2. A pulsed beam structure
   Mu2e has selected an aluminium target where the muon lifetime in the bound system ($\tau_\mu = 864$ ns) well matches the bunch period of the Fermilab accelerator (micro-bunch of 1694 ns period). The trick is to wait for the prompt backgrounds to decay and start the data acquisition $\sim$ 700 ns after the bunch arrival time (Fig. 4).

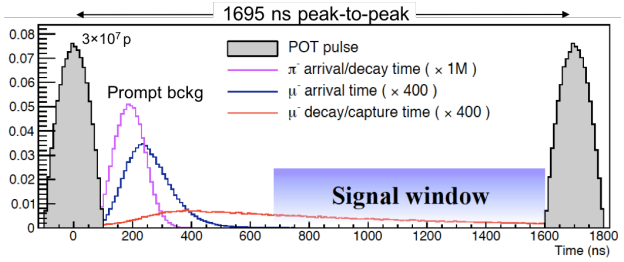

Figure 4. Mu2e bunch structure. The signal window is delayed by 700 ns to allow the decay of the prompt background.

3. A proton extinction better than 10^{-10}
   The number of protons traveling in the beam in the out of time window has to be reduced to the indicated level with respect to the in time protons.

4. A redundant high-precision detector
   This is needed to analyse the products from muon interaction on target to separate CE and DIO spectra and make the contribution from additional background sources negligible.

The layout of the Mu2e experiment is shown in Fig. 5. A series of superconducting solenoids forms a graded magnetic system composed of a Production Solenoid, PS, a Transport Solenoid, TS, and a Detector Solenoid, DS. The PS contains a tungsten target that is struck by an 8 GeV pulsed proton beam. A gradient field in the PS (from 2.5 to 4.6 Tesla) acts as a magnetic lens to focus the produced low energy particles (pions, muons and a small number of antiprotons) into the transport channel. The S-shaped Transport Solenoid efficiently transfers low energy, negatively charged particles to the end of the beamline while allowing a large fraction of pions to decay into muons. Positive and negatively charged particles drift in opposite directions while traveling through the curved solenoidal field, and a mid-section collimator removes nearly all the positively charged particles. The DS uses a graded field from 2 to 1 Tesla in the upstream region where the stopping target resides to increase acceptance for CE events. An uniform magnetic field of 1 Tesla occupies the region of the tracker and calorimeter systems. Approximately 50% of the muon beam, whose momentum is $\sim$ 50 MeV, is stopped by the target; the surviving beam stops on the beam dump at the end of the cryostat. A muon stopping rate of 10 GHz allows the experiment to reach the final goal of 10^{18} stopped muons on target in three years of running. Muons that stop in the aluminium target are captured in an atomic excited state and promptly cascade to the 1S ground state with 39% decaying in orbit and the remaining 61% captured by the nucleus. Low energy photons, neutrons and protons are emitted in the nuclear capture process. These make up an irreducible

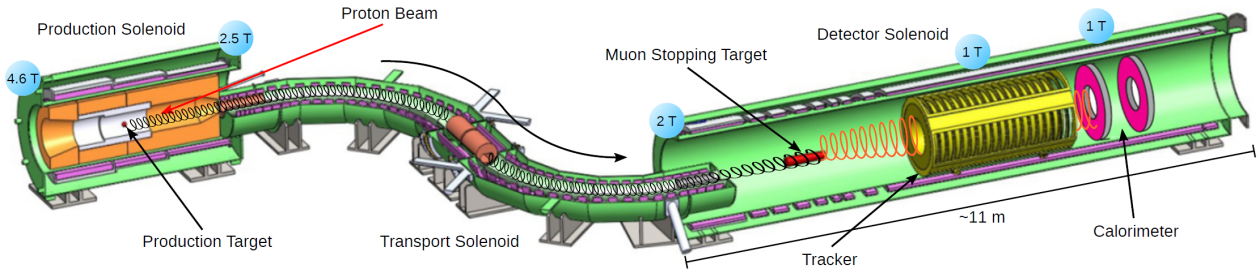

Figure 5. Layout of the Mu2e experiment. The Cosmic Ray Veto, the Extinction Monitor and the Stopping Target Monitor are not shown.

source of accidental activity that is the origin of a large neutron fluence on the detection systems. Together with the flash of particles accompanying the beam, the capture process produces the bulk of the ionizing dose observed in the detector system and its electronics.

The Mu2e tracker is the primary device to measure the momentum of the electron and separate it from background. The crystal calorimeter plays a crucial role in providing particle identification capabilities and a fast online trigger filter, while aiding the track reconstruction capabilities. An external veto for cosmic rays surrounds the solenoid. An extinction monitor detects scattered protons from the production target to evaluate the fraction of out-of-time beam and a stopping target monitor measures the rate and the number of negative muons that stop in the target.

3 Tracker

The Mu2e tracker system [10] has been designed to maximizing acceptance for conversion electrons (CE), minimizing the contamination from the muon Decay-In-Orbit (DIO) background. Nuclear modifications push the DIO spectrum towards the CE signal; energy loss and detector resolution produce overlap of the two processes. The selected design is based on nearly 20,000 low mass straw drift tubes of 5 mm in diameter, with 15 μm Mylar wall and 25 μm sense wire. Straws are oriented transversally to the solenoid axis and arranged in 18 stations for a total lenght of 3.2 metres. A central hole, 38 cm in diameter, makes the device blind to low momentum background particles. (Fig. 6).

Tracker performance has been studied by Monte Carlo using Mu2e full simulation. Results are reported in Fig. 7. The core momentum resolution of 115 keV/c, with a 3% high tail slope of 179 keV/c, is well within physics requirements and stable when incresing accidental hit rate. The total track efficiency of $\sim$ 9% is fully dominated by geometric acceptance.

An eight channel tracker prototype has been built and tested with cosmics. In Fig. 8 the extracted position resolution is compared with Monte Carlo expectations. The shift observed in the transverse resolution is due to the

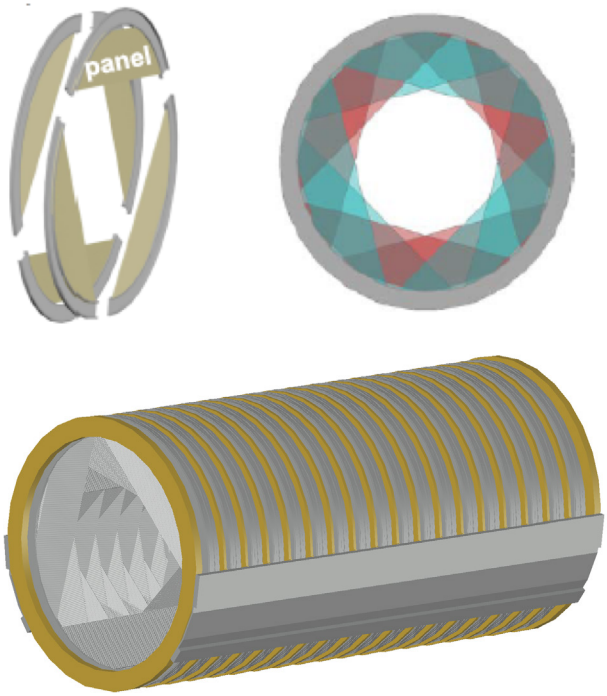

Figure 6. Sketch of the Mu2e straw tracker system. The basic element is the panel, where straws are organized in two staggered layers. Six panels arranged as shown in top-left form a plane; two planes rotated by 30° constitute a station, top-right. The tracker, containing 18 stations, is 3.2 meter long.

T_0 calibration differences. The transverse resolution extracted with a Gaussian fit is (0.133 ± 0.022) mm for data and (0.102 ± 0.001) mm for Monte Carlo simulation. The values extracted for the longitudinal resolution are σ_{data} = (42 ± 1) mm and σ_{MC} = (43 ± 1) mm.

A first pre-production prototype with final design was recently built and is being tested. A vertical slice test on fully instrumented panels with the entire FEE chain will follow.

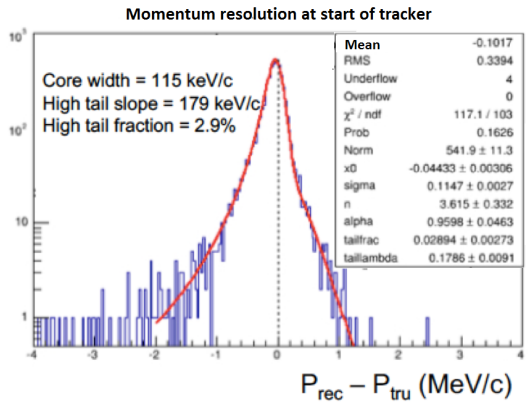

Figure 7. Momentum resolution for conversion electrons obtained with full simulation.

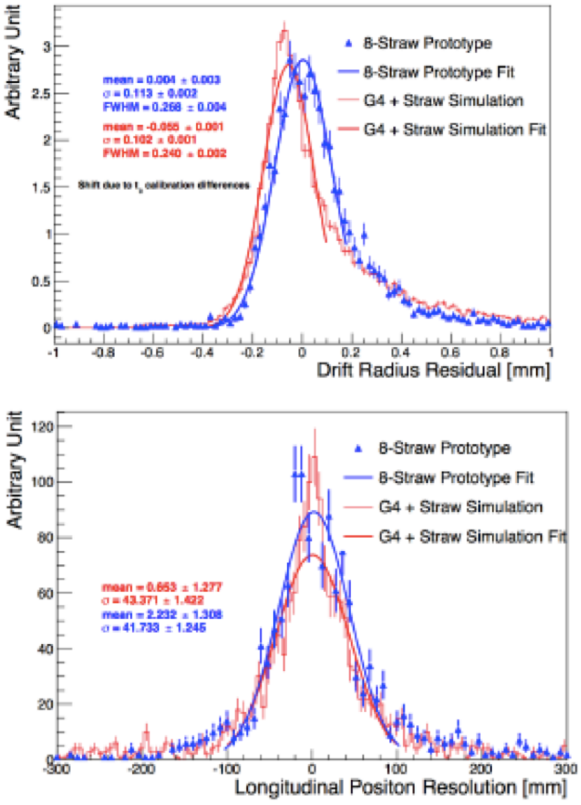

Figure 8. Transverse (top) and longitudinal (bottom) position resolution for an eight channel prototype of the tracker. Data from minimum ionizing particles (blue triangles) are compared with Monte Carlo simulation (red crosses). Resolution is extracted with Gaussian fits to the spectra.

4 Calorimeter

The Mu2e calorimeter [11] has to provide confirmation for CE signal events, a powerful e/μ separation - with a muon rejection factor of ~ 200, a standalone trigger and seeding for track reconstruction. An energy resolution of $O(5\%)$ and a time resolution $<$ 500 ps for 100 MeV electrons

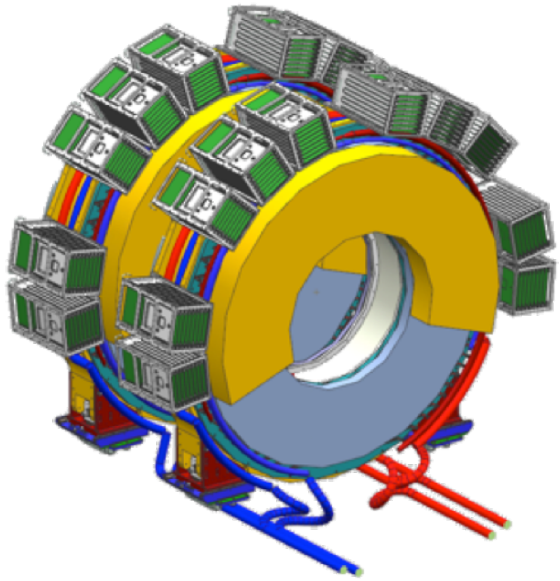

Figure 9. Sketch of the calorimeter system.

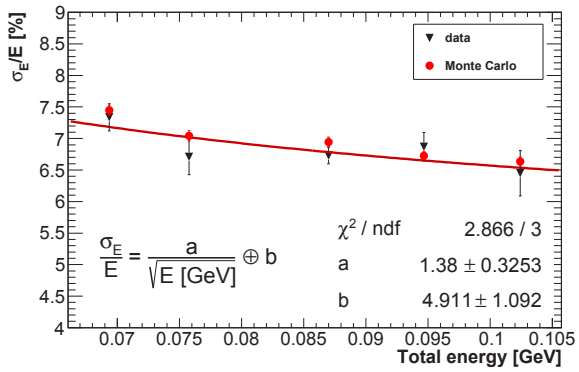

Figure 10. Energy resolution obtained with a (9×9) cm^2 calorimeter prototype.

are sufficient to fulfill these requirements. The calorimeter design consists of two disks made by 674 undoped CsI scintillating crystals with $(34 \times 34 \times 200)$ mm^3 dimension (Fig. 9). Each crystal is read-out by two custom array large area (2×3 of 6×6 mm^2 cells) UV-extended Silicon Photo-Multipliers (SiPMs). The crystals will receive an ionizing dose of 90 krad and a fluence of 3×10^{12} n/cm^2 in three years running. The photosensors, being shielded by the crystals, will get a three times smaller dose.

A small calorimeter protoype, a 3×3 array of CsI crystals coupled to a single multi-pixel photon counter, has been tested at the Frascati Beam Test Facility with electron beams of 80–120 MeV [12]. A time resolution of 100 ps and an energy resolution of 6.5% has been obtained for 100 MeV particles (Figs. 10, 11). For the latter, a significant leakage contribution is present, confirmed by simulation.

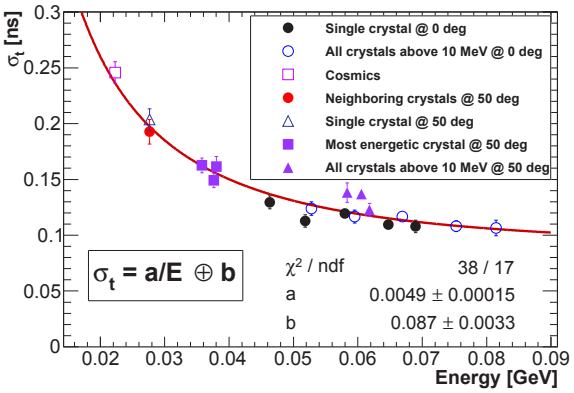

Figure 11. Time resolution obtained with a (9×9) cm^2 calorimeter prototype.

Pre-production components both for crystals and SiPMs have been received from different vendors. They have been characterized and irradiation test have been carried out for a small subsamples. Pre-production components have been used to build a large calorimeter prototype, with 51 crystals and 102 SiPMs and front end boards, testing integration and assembly procedures.

5 Cosmic Ray Veto

The major background source in Mu2e is due to cosmic ray muons that produce fake CE candidates when interacting with the detector materials. These events occur at a rate of approximately one/day. In order to reduce their contributions in the experiment lifetime, the external area of the DS, and a part of the TS, are covered by a Cosmic Ray Veto (CRV) system [7], shown in Fig. 12. The requirement for the CRV system is to obtain a veto efficiency of at least 99.99% for cosmic ray tracks while withstanding an intense radiation environment. Comprised of four staggered layers of scintillation slabs (Fig. 13), the CRV counters are read out with two embedded wavelength shifting fibers, each one in optical contact with a (2×2) mm^2 Hamamatsu SiPM. Test beams on full size prototype have been carried out demonstrating that the needed light yield can be reached [13]: the measured number of photoeletrons obtained at 1 meter from the readout end provides a safety factor of $\sim$ 40% with respect to the requirement. Irradiation of SiPMs with neutrons have also been done to understand the maximum level of fluence acceptable for operations.

6 Expectations with full simulation

At 100 MeV, the momentum resolution is dominated by the fluctuations in the energy loss in the stopping target and bremsstrahlung in the tracker, with the trajectory altered by multiple scattering. The resolution for CE tracks is well-parametrised by a Crystal Ball function with a negative bremsstrahlung tail, a gaussian core of 116 keV and

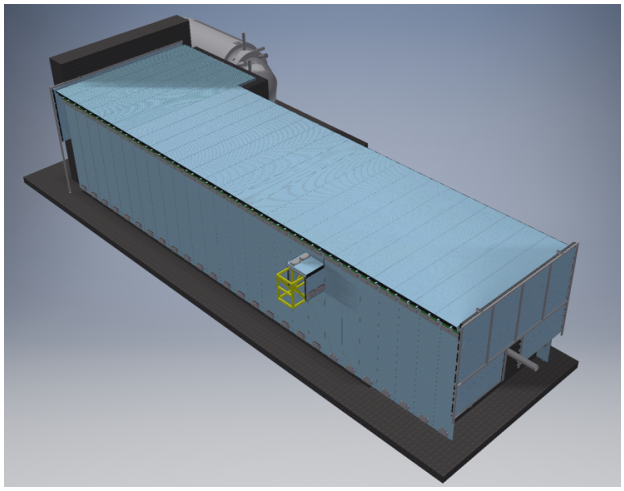

Figure 12. Sketch of the Cosmic Ray Veto.

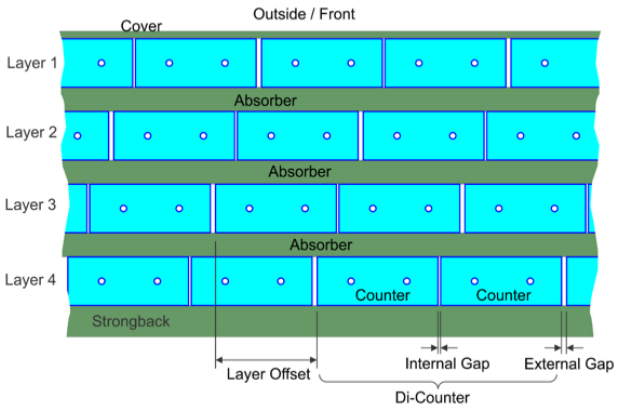

Figure 13. Internal structure of the Cosmic Ray Veto.

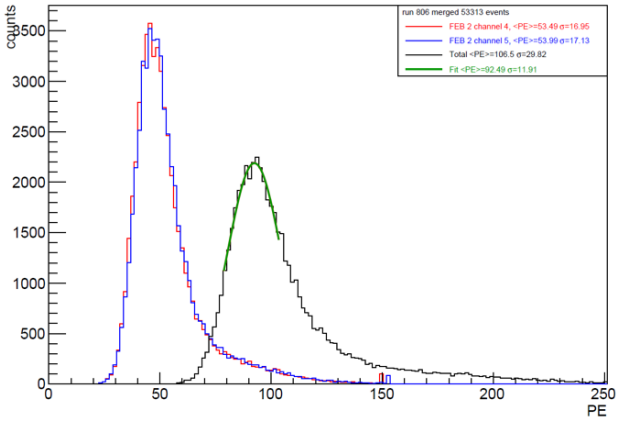

Figure 14. Number of photo-electrons obtained for 120 GeV protons impinging at 1 meter from the readout end. The two peaks are obtained with one (left) and two (right) fiber readout.

a long exponential positive resolution tail. The finite resolution has a large effect on the DIO falling spectrum that translates to a residual contamination in the signal region. Fig. 15 shows the signal and background distributions as

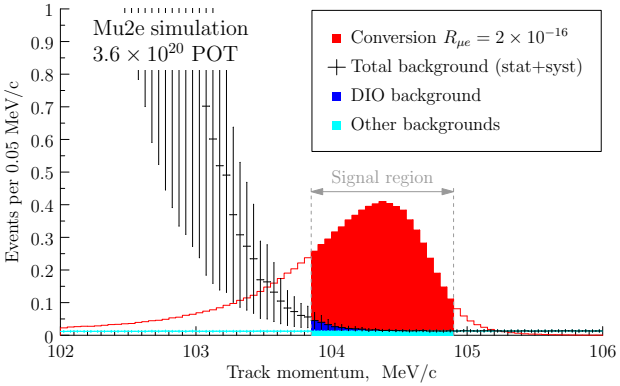

Figure 15. Distribution of the electron momentum spectrum for simulated background and signal events.

seen by a full simulation of the experiment, including pileup, in the following conditions:

- 3.6×10^{20} protons on target;
- a corresponding number of 6×10^{17} muon stops;
- $R_{\mu e}$ of 2×10^{-16}.

A momentum window is selected by maximising the signal over background. The estimate of the background contributions is presented in Table 1, for a total background of 0.46 events. Largest contribution comes from cosmic rays (0.24 events) and DIOs (0.14 events). The number of reconstructed signal events is 6.66. This counting corresponds to set a limit on $R_{\mu e}$ below 8×10^{-17} at 90 % C.L., in good agreement with the design goal of the experiment.

7 Status of the experiment

The Mu2e experiment has, as of this writing, successfully procured all superconducting cables, completed civil construction and obtained CD-3 (Critical Decision 3) from DOE. CD-3 grants permission to start the construction for the accelerator, the magnetic system, the muon beam line and all the detector components. The heart of the Mu2e apparatus is provided by the superconducting magnetic system whose design, fabrication, assembly and commissioning drives the schedule of the experiment. The status of the magnet as well as the construction and testing of the superconducting cables is satisfactory. An international bid for the DS and PS has been concluded and the construction phase for the large magnets is started at General Atomics, San Diego, USA. For the TS, after the construction of one module prototype by ASG Superconducting, in collaboration with the INFN group of Genova, the contract has been awarded to ASG. Construction of the 52 coils is progressing well, with the first 32 already being completed. The first TS module, assembled with two coils, is being delivered and then fully qualified at the HAB test facility in Fermilab. All systems are concluding the prototyping phase. Production of final components is starting, and it will move to full regime by the end of 2017. The schedule foresees a completion of the installation of detectors and commissioning with cosmic rays at the end of 2020.

8 Conclusions

The Mu2e experiment will exploit the world's highest intensity muon beams of the Fermilab Muon Campus to search for CLFV, improving current sensitivity by a factor 10^4 and with a discovery capability over a wide range of New Physics models. A low mass straw tube tracker, a pure CsI crystal calorimeter with SiPM readout and a high efficiency cosmic ray veto have been selected to satisfy the demanding requirements. The construction of the detectors is beginning at the moment of writing. Detector installation is foreseen in 2020, followed by Mu2e commissioning and data taking.

Acknowledgments

We are grateful for the vital contributions of the Fermilab staff and the technical staff of the participating institutions. This work was supported by the US Department of Energy; the Italian Istituto Nazionale di Fisica Nucleare; the US National Science Foundation; the Ministry of Education and Science of the Russian Federation; the Thousand Talents Plan of China; the Helmholtz Association of Germany; and the EU Horizon 2020 Research and Innovation Program under the Marie Sklodowska-Curie Grant Agreement N.690385. Fermilab is operated by Fermi Research Alliance, LLC under Contract No. De-AC02-07CH11359 with the US Department of Energy, Office of Science, Office of High Energy Physics.

References

[1] S. M. Bilenky *et al.*, Phys. Lett. B 67, 309 (1977) 309
[2] F. Grancagnolo *et al.*, Nucl. Phys. Proc. Supp. 248-250 (2014) 1-146.
[3] A. M. Baldini *et al.*, Eur. Phys. J. C 76 (2016) 434.
[4] The SINDRUM II Collaboration, Eur. Phys. J. C 47 (2006) 337-346
[5] A. M. Baldini *et al.*, arXiv:1301.7225 (2013).
[6] A. Blondel *et al.*, arXiv:1301.6113 (2013).
[7] L. Bartoszek *et al.*, "Mu2e Technical Design Report", ArXiv:1501.05241, Fermilab-TM-2594, Fermilab-Design-2014-01.
[8] R. Abramishvili *et al.*, http://comet.kek.jp/Documents_files/PAC-TDR-2016/COMET-TDR-2016_v2.pdf (2016).
[9] H. Natori *et al.*, Nucl. Phys. B Proc. Suppl. 248-250 (2014) 52-57
[10] M. J. Lee on behalf of the Mu2e collaboration, "The Straw-tube Tracker for the Mu2e Experiment", Nuclear and Particle Physics Proceedings 273-275 (2016) 2530.
[11] N.Atanov *et al.*, "Design and status of the Mu2e electromagnetic calorimeter", Nucl. Instr. and Meth. A 824 (2016) 695.

Category	Background process	Estimated Yield (events)
Intrinsic	Decay in orbit (DIO)	0.14 ± 0.11
	Muon Capture (RMC)	0.000 ± 0.004
Late Arriving	Pion capture (RPC)	0.025 ± 0.003
	Muon decay in flight	< 0.003
	Pion decay in flight	$0.000^{+0.001}_{-0.000}$
	beam electrons	$(2.5\pm\ 1.2) \times 10^{-4}$
Miscellaneous	pbar	0.047 ± 0.024
	Cosmic rays	0.24 ± 0.071
	Total	0.46 ± 0.13

Table 1. Expected background list as evaluated by full simulation.

[12] O. Atanova *et al.*, "Measurement of the energy and time resolution of a undoped CsI + MPPC array for the Mu2e experiment", JINST 12 (2017) P05007, ArXiv:1702.03720.

[13] A. Artikov *et al.*, FERMILAB-PUB-17-386-PPD, arXiv:1709.06587, submitted to Nucl. Instr. Meth. A.

[14] G. Blazey *et al.*, "Radiation Tests of Hamamatsu Multi-Pixel Photon Counters", submitted to Nucl. Instr. Meth. A.